ELSEVIER

Materials Science and Engineering B50 (1997) 50–56

MATERIALS SCIENCE & ENGINEERING B

Electrical transport properties of III-nitrides

D.C. Look *

University Research Center, Wright State University, Dayton, OH 45432, USA

Abstract

Excellent n-type GaN layers have been grown by all of the major epitaxial techniques: MBE, MOCVD, and HVPE. In this work, we analyze the band conduction in such samples by temperature-dependent Hall-effect measurement and theory, and determine quantitative information on donor and acceptor concentrations, as well as donor activation energies. In HVPE layers it is necessary to take account of a degenerate n-type layer at the GaN/sapphire interface in order to correctly analyze the bulk material. We also investigate hopping conduction, which occurs at low temperatures in conductive material, and at both low and high temperatures in semi-insulating material. Finally, we show by analysis of electron-irradiation data that both the N vacancy and the N interstitial are electrically active, demonstrating donor and acceptor character, respectively. © 1997 Elsevier Science S.A.

Keywords: Band conduction; Donor activation energies; Hopping conduction

1. Introduction

The recent high activity in the development of GaN epitaxial layers has produced outstanding improvements in quality, with carrier concentrations dropping from $>10^{19}$ to $<10^{17}$ cm^{-3} [1,2], photoluminescence line widths, from >10 to <1 meV [3] and (002) X-ray rocking-curve line widths from several arc min to <30 arc s [4]. These developments are all the more remarkable considering that most of the GaN growth has taken place on a highly mismatched (13.8%) substrate, sapphire. Another indication of high electrical and optical quality is the development of commercial light-emitting diodes as well as prototype laser diodes [5], heterostructure field-effect transistors [6,7], and UV detectors [8]. However, further progress will increasingly depend on a more detailed knowledge of residual defects and impurities, in order to identify and quantify the various donors, acceptors, traps, and recombination centers. The transport properties of semiconductors are strongly influenced by donors and acceptors, both through the carrier concentration and the scattering processes. For good n-type GaN material, in which $n \cong 10^{17}$ cm^{-3}, it is possible to get accurate values of the donor (N_D) and acceptor (N_A) concentrations, and also the donor energy (E_D). For p-type GaN, this task is more difficult, both because the material is of lower quality and because the scattering theory is not as well understood. Finally, for semi-insulating (SI) GaN, hopping transport is dominant and quantitative analyses are nearly impossible. It should be noted that hopping transport is observed at low temperatures in nearly all conductive, nondegenerate samples, but in those cases it is of a simpler nature and can yield quantitative results.

In this work, we will first review n-type scattering theory and the statistical models used to determine carrier concentration. We will then apply these models to GaN layers grown by metal-organic vapor-phase deposition (MOCVD), molecular beam epitaxy (MBE), and hydride vapor-phase epitaxy (HVPE). Various pitfalls which can occur in the Hall analysis of these materials will be discussed. We will then consider the identifications of the donors and acceptors, and show how electron irradiation can be of help in elucidating the electrical activity of defects, in particular, the *N* vacancy and *N* interstitial. Next, we will discuss the dominant transport mechanism in SI GaN, namely hopping conduction, which also occurs in conductive GaN at very low temperatures. Finally, we will briefly review the electrical transport properties of p-type GaN, and of AlN, InN, and their ternary modifications.

* Tel.: +1 937 2551725; fax: +1 937 2553374; e-mail: lookd@el.wpafb.af.mil

PII S0921-5107(97)00163-3

2. Temperature-dependent Hall (TDH) measurements

For over a century, Hall-effect measurements have proven to be a useful way to measure the carrier concentration in semiconductor material, through the relationship $n = r/eR$, where R is the Hall coefficient and r is the Hall factor, usually near unity. In general, the conductivity σ is measured in conjunction with the Hall coefficient, and allows computation of the Hall mobility, $\mu_H = R\sigma$. Since $\sigma = en\mu$, where μ is the conductivity (or drift) mobility, it follows that $\mu = \mu_H/r$. Most workers simply assume $r = 1$, although a few calculate r from μ_H versus temperature T data. However, it is very rare for anyone to actually measure r because of inherent difficulties, and experimental r values have never been obtained in GaN, to our knowledge. We show below that the calculated r's in GaN are typically 1.2–1.4, which thus gives an estimate of the error incurred by assuming $r = 1$.

Our principal objective in performing TDH measurements is to determine donor and acceptor concentrations and their energies with respect to the band edges. For n-type material, we can determine the concentration N_D of the dominant donor (usually the one closest to the Fermi level E_F) and the energy E_D of this donor. Sometimes E_F varies enough as a function of T to reveal two donors, N_{D1} and N_{D2}; however, rarely are three donors recognizable from the n versus T data. The other fitting parameter is the acceptor concentration N_A, but the fitted value of N_A includes all acceptors more than a few kT below E_F. If additional donors N_{DS}, shallower than E_D, also happen to be present, then the fitted parameter is $N_A - N_{DS}$, rather than just N_A. Note that for p-type material, the above discussion holds if the subscripts 'A' and 'D' are simply interchanged.

These ideas are expressed mathematically through the charge balance equation:

$$n + N_A = N_{DS} + \frac{N_D}{1 + n/\phi} \tag{1}$$

where $\phi = (g_0/g_1)N'_C \exp(\alpha/k)T^{3/2} \exp(-E_{D0}/kT)$. Here g_0 is the degeneracy of the unoccupied donor state and g_1 the degeneracy of the occupied state. For an s-like, two-level system, $g_0 = 1$ and $g_1 = 2$. Also, N'_C is the effective density of states at 1 K ($N'_C \cong 4.98 \times 10^{14}$ cm^{-3} for $m^* = 0.22\ m_0$), and α is a temperature coefficient defined by $E_D = E_{D0} - \alpha T$. For two donors, we simply replace the last term by $N_{D1}/(1 + n/\phi_1) + N_{D2}/(1 + n/\phi_2)$. Then, in principle, the fitting parameters would be N_{D1}, N_{D2}, E_{D1}, E_{D2}, α_1, α_2, and N_A. We would expect $\alpha_1 = \alpha_2 \cong 0$ for shallow donors, but even so, there are still five parameters to fit, and it is difficult to get a unique solution in such a case. In practice, we have found that accuracy in N_D and E_D can be achieved if N_A can be fixed, and fortunately, the mobility fit is much more sensitive to N_A than to N_D and E_D. Thus, the key to obtaining accurate values of N_D (or N_{D1} and N_{D2}) and N_A is to first fit N_A from μ versus T data and then fit N_D and E_D from n versus T data.

Mobility fitting is usually accomplished [9] by one of three different methods: (1) Matthiessen's rule; (2) energy averaging; or (3) numerical Boltzmann solution. Method 1, which is the most convenient but least accurate technique, assumes that inverse mobilities add linearly; i.e.

$$\frac{1}{\mu(T)} = \frac{1}{\mu_{ac}(T)} + \frac{1}{\mu_{po}(T)} + \frac{1}{\mu_{pe}(T)} + \frac{1}{\mu_{ii}(T)} \tag{2}$$

where the terms on the right-hand side represent acoustic-mode deformation potential (ac), optic-mode polar potential (po), acoustic-mode piezoelectric potential (pe), and ionized-impurity/defect (ii) scattering, respectively. Expressions for the various terms can be found in Ref. [9]. The second mobility-fitting method assumes that relaxation rates, at a given energy E, add linearly; i.e.

$$\frac{1}{\tau(E,T)} = \frac{1}{\tau_{ac}(E,T)} + \frac{1}{\tau_{po}(E,T)} + \frac{1}{\tau_{pe}(E,T)} + \frac{1}{\tau_{ii}(E,T)} \tag{3}$$

Then, μ is found by a suitable average over energy: $\mu = e\langle\tau\rangle/m^*$ and $\mu_H = e\langle\tau^2\rangle/m^* < \tau >$, where

$$\langle f(\tau)\rangle = \frac{\int_0^\infty f(\tau)E^{3/2}e^{-E/kT}\,dE}{\int_0^\infty E^{3/2}e^{-E/kT}\,dE} \tag{4}$$

for nondegenerate carriers. The problem with this method is that a true closed-form expression for τ_{po} cannot be written, although good approximations are available. Finally, method 3, a numerical solution of the Boltzmann transport (e.g. Rode's iterative method [10]) is the most accurate but also the most computationally intensive. For the best available GaN ($n \cong 10^{17}$ cm^{-3}, $\mu \cong 900$ cm^2 V^{-1} s^{-1}), we have found that methods 2 and 3 give similar values of N_A as long as the high-temperature portion of the μ versus T curve is well fitted by adjusting the scattering strengths of the po and ac mechanisms in each case. The reason is that ii scattering, an elastic mechanism, and thus amenable to method 2, dominates in the low T region, and N_A is the main determinant of the ii scattering strength. However, the μ versus T fit is also used to calculate the Hall factors, $r(T)$, which are necessary to determine $n(T)$, since $n(T) = r(T)/eR(T)$. Method 3 will determine $r(T)$ and thus $n(T)$ more accurately than method 2 in the high T portion of the μ versus T curve, leading to better values of N_D and E_D.

The procedure for getting N_D, E_D and N_A is then as follows:

1. Fit μ versus T and determine N_A and $r(T)$.

2. Calculate $n(T) = r(T)/eR(T)$.
3. Fit n versus T to get N_D and E_D.

In principle, since some of the terms in μ also involve n as well as N_A, we should iterate steps 1 and 2 a few times. That is, we begin step 1 by using n_H as the first estimate, then get n from step 2, then go back to step 1 with this new value of n, etc. However, in practice, the dependence of μ on n is weak enough that it doesn't matter whether n or n_H is used.

3. Application to GaN epitaxial layers

In terms of mobility and surface defect density, the highest-quality GaN produced so far has been grown by the hydride vapor-phase epitaxial (HVPE) technique [11,12]. One of the reasons for this good quality is the fact that an HVPE sample can easily be grown to a large thickness, and thus much of the bulk of the layer is far removed from the high defect interface region. However, all of the HVPE layers that we have studied so far, from two different sources, suffer from a degenerate n-type layer at the GaN/sapphire interface, which does not directly affect the bulk optical and electrical properties, but adds a current shunt which influences the overall measured conductivity and Hall coefficient [13,14]. Fortunately, we can correct for this effect, as shown below.

3.1. Resistivity analysis

It is often instructive to plot resistivity ρ versus $1/T$ in order to get a qualitative picture of electrical behavior. In Fig. 1, we compare ρ versus $1/T$ data for layers grown by HVPE and MOCVD, having respective 300 K mobilities of 785 and 765 $cm^2\ V^{-1}\ s^{-1}$. Beginning at high T (low $1/T$), ρ at first decreases, due to an increase in μ, then ρ increases, due partially to a decrease in μ but mostly due to the electrons freezing out on the donors, and finally ρ increases again but with a much lower activation energy (3.4 meV in this case). The latter behavior is due to hopping conduction, which does not exhibit a Hall effect. All in all, ρ versus T for the MOCVD sample has the classical shape and behavior of a semiconductor material controlled by a shallow donor or acceptor, and is well understood.

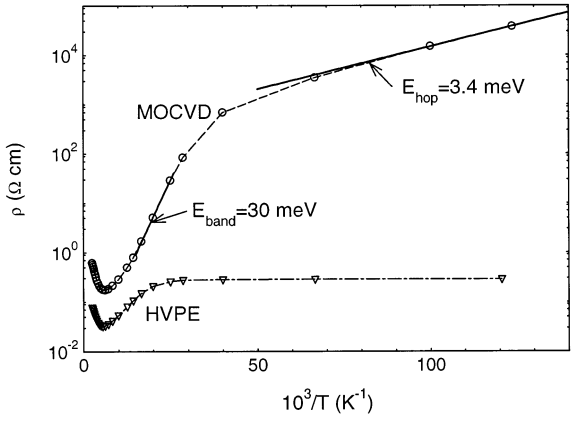

Fig. 1. Resistivity vs. inverse temperature for MOCVD and HVPE GaN on sapphire.

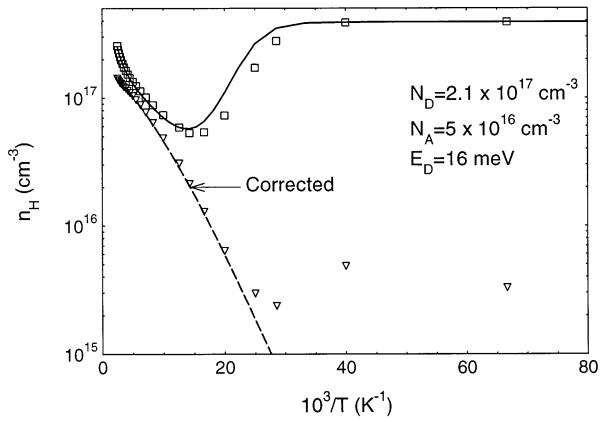

Fig. 2. Uncorrected (for degenerate interface layer) and corrected Hall concentrations for HVPE GaN on sapphire. The solid line is a theoretical fit.

The HVPE layer, while very similar in the high T portion, differs significantly in the low T portion ($10^3/T > 20\ K^{-1}$, or $T < 50$ K). First of all, ρ_{HVPE} is nearly flat (degenerate) in this region, and secondly, it is accompanied by a strong Hall effect. This unusual behavior is due to a thin, degenerate n-type layer at the GaN/sapphire interface, which does not occur in the MOCVD sample.

3.2. Two-layer Hall model

Let the bulk be denoted by layer 1, and the interface, by layer 2. Then it can be shown that

$$\sigma_s = \sigma_{s1} + \sigma_{s2} = e\mu_{H1}n_{Hs1} + e\mu_{H2}n_{Hs2} \quad (5)$$

$$R_s\sigma_s^2 = R_{s1}\sigma_{s1}^2 + R_{s2}\sigma_{s2}^2 = e\mu_{H1}^2 n_{Hs1} + e\mu_{H2}^2 n_{Hs2} \quad (6)$$

where σ_s and R_s are the measured *sheet* conductivity and Hall coefficient, respectively.

It is more convenient to deal with the quantities $\mu_H = R_s\sigma_s$ and $n_H = 1/eR_sd$. Then we can determine the bulk values (layer 1) from the equations

$$\mu_{H1} = \frac{\mu_H^2 n_H - \mu_{H2}^2 n_{Hs2}/d}{\mu_H n_H - \mu_{H2} n_{Hs2}/d} \quad (7)$$

$$n_{H1} = \frac{(\mu_H n_H - \mu_{H2} n_{Hs2}/d)^2}{\mu_H^2 n_H - \mu_{H2}^2 n_{Hs2}/d} \quad (8)$$

where d is the sample thickness. For the HVPE sample shown in Fig. 1, clearly n_{Hs2} and μ_{H2} are constant with temperature, as shown by the squares at low temperatures in Figs. 2 and 3, respectively. That is, $n_{Hs2} =$

$n_{H2}d = (3.9 \times 10^{17}$ cm$^{-3})(20 \times 10^{-4}$ cm$) \cong 8 \times 10^{14}$ cm^{-2}, and $\mu_{H2} \cong 55$ cm^2 V^{-1} s^{-1}. Since n_{Hs2} and μ_{H2} are constant, it is easy to use Eqs. (7) and (8) to correct for the bulk properties over the whole temperature range, and the corrected data are shown as triangles in Figs. 2 and 3.

The solid and dashed lines in Figs. 2 and 3 are theoretical fits to the uncorrected and corrected data, respectively. Here we first fitted μ_{H1} versus T by method 2 (Eq. (4)), described earlier, and obtained $N_A = 5 \times 10^{16}$ cm^{-3}. (The various parameters used in the scattering terms can be found in Ref. [14]). We then fitted n_{H1} versus $1/T$ by Eq. (1) to get $N_D = 2.1 \times 10^{17}$ cm^{-3} and $E_D = 16$ meV. This value of E_D is reasonable, since screening considerations suggest that $E_D = E_{D0} - \beta N_D^{1/3}$, where $\beta \cong 2.1 \times 10^{-5}$ meV cm [15], and if the donor is Si, then $E_{D0} \cong 29$ meV [16], giving a predicted value of $E_D = 16.5$ meV at $N_D = 2.1 \times 10^{17}$ cm^{-3}.

Note that if we had not corrected the n_H data, and had fitted only the portion at $T > 80$ K, which is the common procedure, then we would have had to use a two-donor model. That is, the uncorrected n_H data in Fig. 2 clearly show a strong upturn at high T, which would naturally be interpreted as a deeper donor. Thus, the low T data are critical in revealing the degenerate layer. To allay the fears of those who have fitted Hall curves in the past, we may note that, so far, we have not found any MOCVD or MBE layers that have exhibited a strong, degenerate interface layer. Evidently the usual AlN or GaN prelayers grown at low temperatures in these latter methods help prevent a degenerate interface.

4. Identification of donors and acceptors

Early studies of GaN, which nearly always involved materials with high donor concentrations [1], concluded

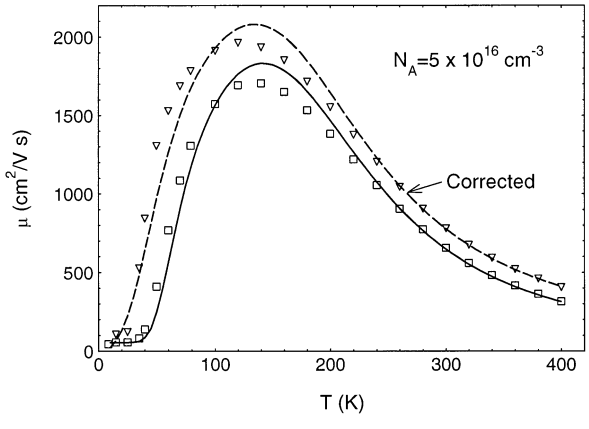

Fig. 3. Uncorrected (for degenerate interface layer) and corrected Hall mobilities for HVPE GaN on sapphire. Both the solid and dashed lines are theoretical fits assuming $N_A = 5 \times 10^{16}$ cm^{-3}.

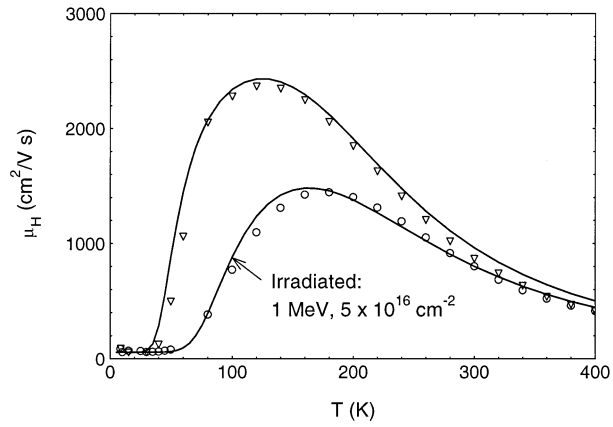

Fig. 4. Uncorrected Hall mobilities for unirradiated (triangles) and irradiated (circles) HVPE GaN layers on sapphire. The solid lines are theoretical fits.

that the dominant donor was the nitrogen vacancy V_N [17], and many later investigations have agreed with this identification [18]. However, strong arguments for oxygen [19,20] and silicon [21] as residual donors have also been advanced. The only potential residual acceptor which has received much attention is the gallium vacancy, V_{Ga} [20,22]. Since the gallium interstitial Ga_I should also be a donor [18,23], it is quite important to firmly establish which, if any, of the point defects in GaN have donor or acceptor nature. Recent electron-irradiation studies [12,24] help to elucidate this matter.

High-energy electrons (say, at 1 MeV) knock atoms out of their lattice positions and create Frenkel (vacancy-interstitial) pairs. If the interstitials can move at the irradiation temperature (about 300 K, in our case), then the crystal can end up with a variety of defects, including Frenkel pairs, isolated vacancies, interstitial complexes, and possibly antisites. Some of these possibilities can be eliminated by annealing experiments; e.g. a Frenkel pair will anneal by first-order kinetics, whereas most of the other defects will anneal by second-order or higher kinetics. The multiplicity of potential defects is of course increased in a compound semiconductor, because both sublattices can be involved.

We have irradiated a 60-μm-thick HVPE GaN layer on sapphire with 1 MeV electrons from a van de Graaff accelerator. This sample exhibited a near-record mobility of about 950 cm^2 V^{-1} s^{-1} at 300 K, after correction for the degenerate interface layer usually found in HVPE GaN on sapphire. The range of 1 MeV electrons in GaN is about 700 μm, so little energy loss occurs in a 60-μm-thick sample. The change in mobility after an irradiation fluence $F = 5 \times 10^{16}$ electrons cm^{-2} is shown in Fig. 4. The solid lines are theoretical fits which give an increase in N_A from 3 to 8×10^{16} cm^{-3}. In other words, $\Delta N_A = 5 \times 10^{16}$ cm^{-3}, or the acceptor production rate is $\tau_A = \Delta N_A / \Delta F \cong 1$ cm^{-1}. The uncor-

rected carrier concentrations for the unirradiated and irradiated samples are shown in Fig. 5. Here, the theoretical fits show that a new donor, of concentration 5×10^{16} cm^{-3} and energy 64 meV, is introduced by the irradiation, thus, $\tau_D \cong 1$ cm^{-1}. These values of τ_A and τ_D are equal, within error, which suggests that the irradiation mainly creates N Frenkel pairs, V_N–N_I, in which V_N is a donor, as expected, and N_I is an acceptor, as predicted by theory [22,23] but still quite surprising. Thermal annealing of the damage occurs at 300–350°C, and can be well fitted by first-order kinetic theory [12] which supports the N Frenkel-pair model. Possible Ga Frenkel-pair production is not supported by the data, because V_{Ga} is a triple acceptor in GaN [22,23], which would appear to give three times as many acceptors as donors. Also, the energy dependence of τ agrees with the N model but not the Ga model.

Interestingly, the energy E_D of the created donor V_N is about 60–70 meV—much higher than the 16 meV measured for the original (residual) donor. Thus, it seems that V_N is shallow, but not purely hydrogenic. This conclusion, while not surprising, needs to be verified in more samples. If true, it reveals that most of the high-quality ($n \leq 10^{17}$ cm^{-3}) GaN layers studied recently, which typically have E_D's less than 30 meV, have a *residual* donor other than V_N. However, some of the bulk-grown crystals, which are probably Ga-rich and exhibit high values of n, may well have V_N donors. With regard to the N_I acceptors, it is interesting that increasingly N-rich MBE GaN layers go from strongly n-type ($n \cong 10^{18}$ cm^{-3}) to semi-insulating [25]. It is possible that the N_I centers, which are thought to have acceptor levels at about $E_V + 1.0$ eV [23], may play a role in the compensation of these particular SI MBE layers.

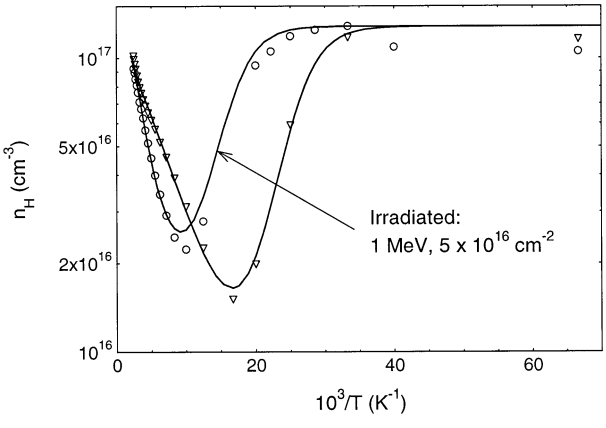

Fig. 5. Uncorrected Hall concentrations for unirradiated (triangles) and irradiated (circles) HVPE GaN on sapphire. The solid lines are theoretical fits.

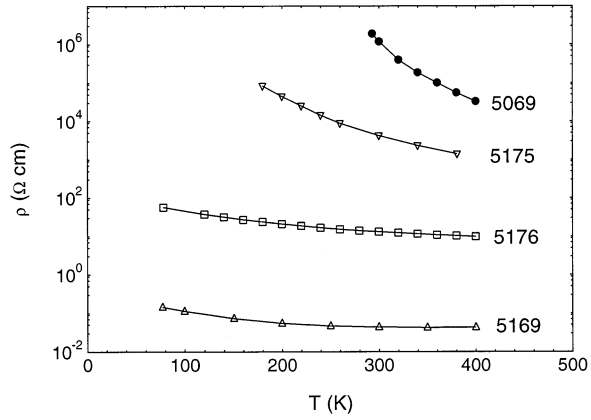

Fig. 6. Resistivity vs. temperature for MBE GaN on sapphire. The higher resistivities correspond to higher N fluxes during growth.

5. Semi-insulating GaN

Although as-grown GaN is normally n-type, it can be made semi-insulating (SI) either by doping with acceptors, such as Zn [26], or by control of stoichiometry in both MBE [25] and MOCVD [27] growth. The resistivities of four layers grown by reactive MBE with different N fluxes are shown in Fig. 6 [25]. The more resistive layers were grown at higher N fluxes. Sample 5169 was strongly conductive, with $n \cong 10^{18}$ cm^{-3}, while samples 5175 and 5069 exhibited no Hall effect, i.e. $\mu_H < 1$ cm^2 V^{-1} s^{-1}. This situation is in stark contrast to that of SI GaAs, which has even higher resistivity ($\rho \geq 10^7$ Ω cm) but yet shows a strong Hall effect ($\mu_H \geq 7000$ cm^2 V^{-1} s^{-1}). It is known that hopping conduction generally has no Hall effect, as indeed is the case for the low T data of the MOCVD sample shown in Fig. 1. Thus, it is natural to assign the transport mechanism of SI-GaN samples 5175 and 5069 to hopping. However, the temperature dependences of ρ for these samples are much stronger than that of the MOCVD sample in Fig. 1, which had $E_{hop} = 3.4$ meV. For example, on a $\ln(\rho)$ versus $1/T$ plot, the slope of the sample 5069 data gives $E_{hop} = 380$ meV. Thus, a hop in the MOCVD sample can take place by interaction with a single acoustic phonon, whereas a hop in the MBE sample must involve many phonons. A plot of $\ln(\rho)$ versus $1/T^{1/4}$ (not shown) is a reasonably straight line [25]; thus, we can write

$$\sigma_{hop} = Ce^{-(T_0/T)^{1/4}} \tag{9}$$

where $T_0 \cong 1.8 \times 10^6$ K. Usually, this type of temperature dependence is assigned to single-phonon, variable-range hopping [28,29], but Emin has shown that the same behavior can result from multiphonon hopping, at least over a certain temperature range. These data are discussed in Ref. [25], but our understanding of hopping mechanisms among deep centers in GaN is still in its infancy.

6. p-Type GaN

It is generally acknowledged that the rapidly developing interest in GaN and related materials over the last few years is due to the development of p-type layers [30]. However, the electrical characteristics of p-type GaN are still quite poor compared to those of n-type GaN. For example, typical results for wurtzitic, p-type GaN are analyzed in Ref. [31]. The 300 K mobility is only about 10 $cm^2\ V^{-1}\ s^{-1}$ at a hole concentration of about $10^{17}\ cm^{-3}$. Actually, the acceptor (Mg) doping is much higher, about $2 \times 10^{19}\ cm^{-3}$, but the 0.17 eV activation energy of Mg is responsible for the fact that $p \ll N_A$.

Rubin et al. [32], using a Kaufman ion gun to produce an N_2^+ source, report a 300 K hole mobility of 12 $cm^2\ V^{-1}\ s^{-1}$ for an Mg-doped layer with $p = 2 \times 10^{16}\ cm^{-3}$. Surprisingly, however, for an undoped layer, grown with a high N_2^+ flux, they get a 300 K mobility of about 150 $cm^2\ V^{-1}\ s^{-1}$, but at a very low hole concentration, $p \cong 4 \times 10^{12}\ cm^{-3}$. For this sample, the dominant acceptor had an activation energy of 0.29 eV, much deeper than that of Mg.

Higher hole mobilities have been found in cubic GaN. An MBE sample grown on GaAs and co-doped with Be and O exhibited a 300 K mobility of 150 $cm^2\ V^{-1}\ s^{-1}$ at a very high hole concentration, $p = 1 \times 10^{18}\ cm^{-3}$ [33], and another MBE layer on GaAs produced an even higher mobility, 350 $cm^2\ V^{-1}\ s^{-1}$, although with p only about $10^{13}\ cm^{-3}$ [34]. These results are promising and indicate that cubic GaN may have an advantage with respect to p doping; however, much more work needs to be done in this area.

7. Transport in AlN, AlGaN, InN, InGaN, and AlInN

Gaskill, Rowland, and Doverspike have well summarized the transport properties of AlN, GaN, and AlGaN [35], and Bryden and Kistenmacher have done the same for InN, InGaN, and AlInN [36]. Unfortunately, much less work has been carried out in these materials than in GaN, and results are sometimes conflicting. In general, undoped AlN and $Al_xGa_{1-x}N$, with $x > 0.4$, are insulating materials, and doping is difficult. On the other hand, InN is normally n-type and highly conductive. Detailed information and further references on materials such as these can be found in the works cited above.

8. Summary

Electrical transport in n-type GaN is fairly well understood at the present time. Quantitative measures of donors and acceptors can be obtained and the electrical properties of several different dopants and also two intrinsic defects have been elucidated. However, the situation is not the same in p-type GaN: reported mobilities are generally lower than expected, and very little serious work on hole scattering theory has been attempted. Even less is understood about transport in some of the other III-nitrides, such as AlN, InN, and the (Ga, Al, In)N ternaries. However, knowledge of these materials is increasing at a rapid pace because of their technological importance.

Acknowledgements

I would like to thank several colleagues for stimulating discussions on the III-nitrides: Z.-Q. Fang, R.L. Jones, C.W. Litton, R.J. Molnar, H. Morkoç, D.C. Reynolds, J.R. Sizelove, and C.E. Stutz. I also much appreciate the assistance of Nalda Blair in the manuscript preparation. Finally, I would like to acknowledge the support of the US Air Force, under Contract F33615-95-C-1619, and DARPA, under Contract F33615-95-C-1751. Most of my work was performed at the Avionics Directorate, Wright Laboratory.

References

[1] R. Dingle, D.D. Sell, S.E. Stokowski, P.J. Dean, R.B. Zetterstrom, Phys. Rev. B 3 (1971) 1211.
[2] S. Nakamura, T. Mukai, M. Senoh, J. Appl. Phys. 71 (1992) 5543.
[3] T. Suski, P. Perlin, M. Leszczynski, et al., Mater. Res. Soc. Symp. Proc. 395 (1996) 15.
[4] A. Saxler, M.A. Capano, W.C. Mitchel, et al., Mater. Res. Soc. Symp. Proc. 449 (1997) 477.
[5] S. Nakamura, Mater. Res. Soc. Symp. Proc. 449 (1997) 1135.
[6] J. Burm, K. Chu, W.J. Schaff, et al., IEEE Electron Device Lett. 18 (1997) 141.
[7] F. Stengel, S.N. Mohammed, H. Morkç, J. Appl. Phys. 80 (1996) 3031.
[8] M. Razeghi, A. Rogalski, J. Appl. Phys. 79 (1996) 7433.
[9] D.C. Look, Electrical Characterization of GaAs Materials and Devices, Wiley, New York, 1989.
[10] D.L. Rode, Semicond. Semimet. 10 (1975) 1.
[11] R.J. Molnar, K.B. Nichols, P. Makai, E.R. Brown, I. Melngailis, Mater. Res. Soc. Symp. Proc. 378 (1995) 479.
[12] D.C. Look, D.C. Reynolds, J.W. Hemsky, J.R. Sizelove, R.L. Jones, R.J. Molnar, Phys. Rev. Lett. 79 (1997) 2273.
[13] W. Götz, J. Walker, L.T. Romano, N.M. Johnson, R.J. Molnar, Mater. Res. Soc. Symp. Proc. 449 (1997) 525.
[14] D.C. Look, R.J. Molnar, Appl. Phys. Lett. 70 (1997) 3377.
[15] B.K. Meyer, D. Volm, A. Graber, et al., Solid State Commun. 95 (1995) 597.
[16] Y.J. Wang, R. Kaplan, H.K. Ng, et al., J. Appl. Phys. 79 (1996) 8007.
[17] H.P. Maruska, J.J. Tietjen, Appl. Phys. Lett. 15 (1969) 327.
[18] P. Perlin, T. Suski, H. Teisseyre, et al., Phys. Rev. Lett. 75 (1995) 296.
[19] B.-C. Chung, M. Gershenzon, J. Appl. Phys. 72 (1992) 651.

[20] C.G. Van de Walle, J. Neugebauer, Mater. Res. Soc. Symp. Proc. 449 (1997) 861.
[21] W. Götz, N.M. Johnson, C. Chen, H. Liu, C. Kuo, W. Imler, Appl. Phys. Lett. 68 (1996) 3144.
[22] J. Neugebauer, C.G. Van de Walle, Phys. Rev. B 50 (1994) 8067.
[23] P. Boguslawski, E.L. Briggs, J. Bernholc, Phys. Rev. B 51 (1995) 17255.
[24] M. Linde, S.J. Uftring, G.D. Watkins, V. Härle, F. Scholz, Phys. Rev. B 55 (1997) 10177.
[25] D.C. Look, D.C. Reynolds, W. Kim, et al., J. Appl. Phys. 80 (1996) 2960.
[26] H. Amano, K. Hiromatsu, M. Kitto, N. Sawaki, I. Akasaki, J. Cryst. Growth 93 (1988) 79.
[27] K. Doverspike, A.E. Wickenden, S.C. Binari, D.K. Gaskill, J.A. Freitas, Mater. Res. Soc. Symp. Proc. 395 (1996) 897.
[28] N.F. Mott, W.D. Twose, Adv. Phys. 10 (1961) 107.
[29] B.I. Shklovskii, Sov. Phys. Semicond. 6 (1973) 1053.
[30] H. Amano, M. Kito, K. Hiamatsu, I. Akasaki, Jpn. J. Appl. Phys. 28 (1989) L2112.
[31] H. Nakayama, P. Hacke, M.R.H. Khan, T. Detchprohm, K. Hiramatsu, N. Sawaki, Jpn. J. Appl. Phys. 35 (1996) L282.
[32] M. Rubin, N. Newman, J.S. Chan, T.C. Fu, J.T. Ross, Appl. Phys. Lett. 64 (1994) 64.
[33] O. Brandt, H. Yang, H. Kostial, K.H. Ploog, Appl. Phys. Lett. 69 (1996) 2707.
[34] D.J. As, D. Schikora, A. Greiner, M. Lubbers, J. Mimkes, K. Lischka, Phys. Rev. B 54 (1996) R11118.
[35] D.K. Gaskill, L.B. Rowland, K. Doverspike, in: J.H. Edgar (Ed.), Properties of Group III Nitrides, INSPEC, London, 1994, p. 101.
[36] W.A. Bryden, T.J. Kistenmacher, in: J.H. Edgar (Ed.), Properties of Group III Nitrides, INSPEC, London, 1994, p. 117.